J|A|C|S
ARTICLES
Published on Web 03/19/2002

Proton Transfer Reactions on Semiconductor Surfaces

Collin Mui,[†] Joseph H. Han,[†] George T. Wang,[†] Charles B. Musgrave,[†,‡] and Stacey F. Bent*,[†]

Contribution from the Department of Chemical Engineering, Stanford University, Stanford, California 94305-5025, and Department of Materials Science and Engineering, Stanford University, Stanford, California 94305-2205

Received September 24, 2001

Abstract: The concept of proton affinity on semiconductor surfaces has been explored through an investigation of the chemistry of amines on the Ge(100)-2 × 1, Si(100)-2 × 1, and C(100)-2 × 1 surfaces. Multiple internal reflection Fourier transform infrared (MIR-FTIR) spectroscopy, temperature programmed desorption (TPD), and density functional theory (DFT) calculations were used in the studies. We find that methylamine, dimethylamine, and trimethylamine undergo molecular chemisorption on the Ge(100)-2 × 1 surface through the formation of Ge−N dative bonds. In contrast, primary and secondary amines react on the Si(100)-2 × 1 surface via N−H dissociation. Since N−H dissociation of amines at semiconductor surfaces mimics a proton-transfer reaction, the difference in chemical reactivities of the Ge(100)-2 × 1 and Si(100)-2 × 1 surfaces toward N−H dissociation can be interpreted as a decrease of proton affinity down a group in the periodic table. The trend in proton affinities of the two surfaces is explained in terms of thermodynamics and kinetics. Solid-state effects on the C(100)-2 × 1 surface and the surface proton affinity concept are discussed based on our theoretical predictions.

Introduction

The systematic arrangement of the periodic table allows us to predict not only the physical properties but also the chemical reactivities of the elements. One periodic property of the nonmetals is that the proton affinity or the basicity of the element decreases down a group. In group V-A, for example, it is well-known that ammonia (NH_3) is a relatively strong base that combines readily with a proton to form the ammonium ion (NH_4^+) in aqueous solution, whereas the formation of the phosphonium ion (PH_4^+) from phosphine (PH_3) is unfavorable under similar conditions.[1] The gas-phase proton affinity of arsine (AsH_3) is even weaker than that of PH_3.[2]

The periodic trend in the lone pair basicity of group V hydrides provides a chemical model for the reactivity of lone pairs of other molecules. For example, the same group trend is also observed for the proton affinity of group IV-A anionic hydrides,[1] in which the base strengths of the anions follow the order CH_3^- > SiH_3^- > GeH_3^-. Interestingly, group IV semiconductor surfaces also comprise a chemical system that appears to follow this group trend in lone pair proton affinity. The proton affinity in this case can be examined due to the zwitterionic nature of the surfaces in which the surfaces consist of electrophilic and nucleophilic sites with direct analogies to molecular systems.

The reconstruction of the (100) semiconductor surface is responsible for the presence of electrophilic and nucleophilic sites. The clean (100) surfaces of diamond, silicon, and germanium single crystals undergo a 2 × 1 reconstruction, in which rows of dimers are formed between the surface atoms.[3] Due to the solid-state electronic structure of these materials, the C(100)-2 × 1 surface consists of symmetric dimers;[4,5] asymmetric dimers are stable on the Si(100)-2 × 1 surface at low temperatures;[6,7] and the dimers of the Ge(100)-2 × 1 surface are statically buckled even at room temperature.[8] In each case, however, the bonding between the two atoms of a surface dimer involves a strong σ-bond and a weak π-bond. The dimer bond of a tilted dimer deviates from the plane of the surface, and the resulting structure of each dimer consists of an "up" dimer atom protruding from the surface and a "down" dimer atom recessed on the surface. The dangling bond of the up atom has more s-orbital character than the bulk sp^3 bonds while the dangling bond of the down atom has more p-orbital character.[9] Hence, the electron density at the up atom of the dimer is higher than that at the down atom. A direct consequence of the charge asymmetry is that the down atom becomes electrophilic and the up atom becomes nucleophilic. The down atom hence can act as an electron acceptor and participate in electron-transfer reactions such as Lewis acid−base reactions. In contrast, the

* Address correspondence to this author. E-mail: stacey.bent@stanford.edu.
[†] Department of Chemical Engineering, Stanford University.
[‡] Department of Materials Science and Engineering, Stanford University.

(1) Wulfsberg, G. *Principles of Descriptive Inorganic Chemistry*; University Science Books: Mill Valley CA, 1991.
(2) Hunter, E. P. L.; Lias, S. G. *J. Phys. Chem. Ref. Data* **1998**, *27*, 413−656.
(3) Duke, C. B. *Chem. Rev.* **1996**, *96*, 1237−1259.
(4) Thoms, B. D.; Butler, J. E. *Surf. Sci.* **1995**, *328*, 291−301.
(5) Mercer, T. W.; Pehrsson, P. E. *Surf. Sci.* **1998**, *399*, L327−L331.
(6) Hamers, R. J.; Tromp, R. M.; Demuth, J. E. *Phys. Rev. B* **1986**, *34*, 5343−5357.
(7) Hata, K.; Yasuda, S.; Shigekawa, H. *Phys. Rev. B* **1999**, *60*, 8164−8170.
(8) Kubby, J. A.; Griffith, J. E.; Becker, R. S.; Vickers, J. S. *Phys. Rev. B* **1987**, *36*, 6079−6093.
(9) Konecny, R.; Doren, D. J. *J. Chem. Phys.* **1997**, *106*, 2426−2435.

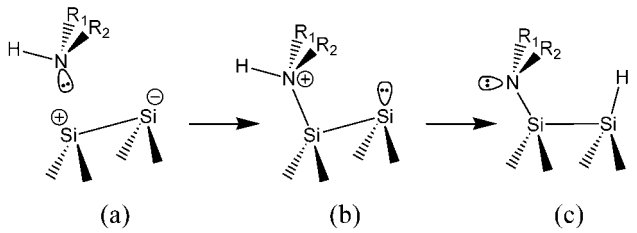

Figure 1. An illustration of the surface reaction of an amine at the Si(100)-2 × 1 surface, in which a quaternary ammonium ion is formed upon initial adsorption. The subsequent N−H dissociation reaction is analogous to a proton transfer at the surface.

up atom resembles a lone pair that can act as a Lewis base and participate in proton-transfer reactions.

Dissociative adsorption of amines[10−15] at the surface dimers provides an excellent system to probe proton-transfer affinities of the three elemental surfaces. Amines contain nitrogen lone pair electrons that can interact with the electrophilic down atom of a tilted dimer to form a dative bond via a Lewis acid−base interaction, as illustrated for the Si(100)-2 × 1 surface in Figure 1a. Upon initial adsorption of the amine, the up atom of the dimer, being electron rich, resembles a nucleophilic surface site, depicted in Figure 1b. The dative bonded adsorbed state can be viewed as a quaternary ammonium ion at the surface. In the case of primary and secondary amines, the complex has the possibility of undergoing N−H dissociation from the adsorbed state. The N−H dissociation process is analogous to an intradimer proton-transfer reaction since it involves the abstraction of a proton from the quaternary ammonium ion by the nucleophilic up atom of the tilted dimer. The final surface reaction product after dissociation is shown in Figure 1c.

The notion of proton-transfer reactions at semiconductor surfaces is proposed based on our study of N−H dissociation reactions at the Si(100)-2 × 1 surface.[13] The reaction on the Si(100)-2 × 1 surface was described as an intradimer proton transfer based on two pieces of evidence. First, orbital overlap analysis during N−H dissociation shows that electron density is being transferred from the amine lone pair to the nucleophilic Si atom upon initial adsorption of the amine molecule. The transition state involves electron donation from the nucleophilic Si atom to the N−H σ-antibonding orbital. After the transition state, electron density reappears only at the N atom and regenerates the lone pair. In summary, little electron density is associated with the hydrogen during the dissociation process, hence the dissociating hydrogen resembles a proton more than a neutral H atom.

The second piece of evidence for the proton-transfer description is based on the reaction energetics of N−H dissociation on the Si(100)-2 × 1 surface. Specifically, we find energetic trends more closely aligned with transfer of a proton than transfer of a neutral H atom. The calculated adsorption energy of ammonia and methylamines via N−H dissociation on the Si(100)-2 × 1 surface becomes less exothermic as the number of methyl groups in the amine molecule increases. Similarly, gas-phase proton affinity of ammonia increases with methyl substitution, whereas the homolytic N−H bond energy of ammonia follows the opposite trend, decreasing with increasing methyl substitution. Thus, N−H dissociative adsorption of amine on the Si(100)-2 × 1 surface follows the energetic characteristics of proton-transfer reactions, lending further support for this reaction model.

In the present study we explore the chemistry of amines at the Ge(100)-2 × 1 surface, and make theoretical predictions about the diamond(100)-2 × 1 surface, which allows us to investigate periodic trends in proton affinity. We will show that there are significant differences in the surface chemistry of methylamines at the Ge(100)-2 × 1 and Si(100)-2 × 1 surfaces. In contrast to the Si(100)-2 × 1 surface, we find that methylamine, dimethylamine, and trimethylamine all undergo molecular chemisorption on the Ge(100)-2 × 1 surface through the formation of surface Ge−N dative bonds, and subsequent N−H dissociation of the amines is not observed. Our combined experimental and theoretical results imply that the proton affinity of the nucleophilic up atom of a Ge−Ge dimer is lower than that of a Si−Si dimer.

This study of the periodic trend of proton transfer chemistry in group IV materials provides additional support for treating semiconductor surface reactivities within a localized molecular framework. This molecular approach has been applied successfully to understand reactions of unsaturated hydrocarbons at such surfaces by analogy to cycloaddition chemistry. For example, it has been shown that the dimers on the C(100)-2 × 1, Si(100)-2 × 1, and Ge(100)-2 × 1 surfaces, which contain a weak π-bond as well as a σ-bond, undergo cycloaddition reactions with unsaturated hydrocarbons.[16−26] While these previous studies are focused on drawing analogies and exploiting similarities of group IV semiconductor surfaces, the current study reveals some of the differences and highlights trends in chemical reactivity between silicon and germanium.

Experimental Details

The experimental approach was based on spectroscopic studies performed under ultrahigh vacuum (UHV) conditions. Multiple internal reflection Fourier transform infrared (MIR-FTIR) spectroscopy was used to identify the surface reaction products between methylamine, dimethylamine, and trimethylamine and the Si(100)-2 × 1 and Ge(100)-2 × 1 surfaces. The thermal desorption behavior of the amines on the Ge(100)-2 × 1 surface was studied using temperature-programmed desorption (TPD). MIR-FTIR and TPD experiments were performed in two different UHV systems.

Infrared spectroscopy experiments were performed in a UHV chamber with a base pressure less than 1.0×10^{-9} Torr, described in

(10) Mulcahy, C. P. A.; Carman, A. J.; Casey, S. M. *Surf. Sci.* **2000**, *459*, 1−13.
(11) Cao, X. P.; Coulter, S. K.; Ellison, M. D.; Liu, H. B.; Liu, J. M.; Hamers, R. J. *J. Phys. Chem. B* **2001**, *105*, 3759−3768.
(12) Wang, G. T.; Mui, C.; Musgrave, C. B.; Bent, S. F. *J. Phys. Chem. B* **2001**, *105*, 3295−3299.
(13) Mui, C.; Wang, G. T.; Bent, S. F.; Musgrave, C. B. *J. Chem. Phys.* **2001**, *114*, 10170−10180.
(14) Luo, H. B.; Lin, M. C. *Chem. Phys. Lett.* **2001**, *343*, 219−224.
(15) Cao, X. P.; Hamers, R. J. *J. Am. Chem. Soc.* **2001**, *123*, 10988−10996.
(16) Wang, G. T.; Bent, S. F.; Russell, J. N.; Butler, J. E.; D'Evelyn, M. P. *J. Am. Chem. Soc.* **2000**, *122*, 744−745.
(17) Hovis, J. S.; Coulter, S. K.; Hamers, R. J.; D'Evelyn, M. P.; Russell, J. N.; Butler, J. E. *J. Am. Chem. Soc.* **2000**, *122*, 732−733.
(18) Fitzgerald, D. R.; Doren, D. J. *J. Am. Chem. Soc.* **2000**, *122*, 12334−12339.
(19) Teplyakov, A. V.; Kong, M. J.; Bent, S. F. *J. Am. Chem. Soc.* **1997**, *119*, 11100−11101.
(20) Teplyakov, A. V.; Kong, M. J.; Bent, S. F. *J. Chem. Phys.* **1998**, *108*, 4599−4606.
(21) Hamers, R. J.; Hovis, J. S.; Lee, S.; Liu, H. B.; Shan, J. *J. Phys. Chem. B* **1997**, *101*, 1489−1492.
(22) Konecny, R.; Doren, D. J. *J. Am. Chem. Soc.* **1997**, *119*, 11098−11099.
(23) Konecny, R.; Doren, D. J. *Surf. Sci.* **1998**, *417*, 169−188.
(24) Choi, C. H.; Gordon, M. S. *J. Am. Chem. Soc.* **1999**, *121*, 11311−11317.
(25) Teplyakov, A. V.; Lal, P.; Noah, Y. A.; Bent, S. F. *J. Am. Chem. Soc.* **1998**, *120*, 7377−7378.
(26) Lee, S. W.; Hovis, J. S.; Coulter, S. K.; Hamers, R. J.; Greenlief, C. M. *Surf. Sci.* **2000**, *462*, 6−18.

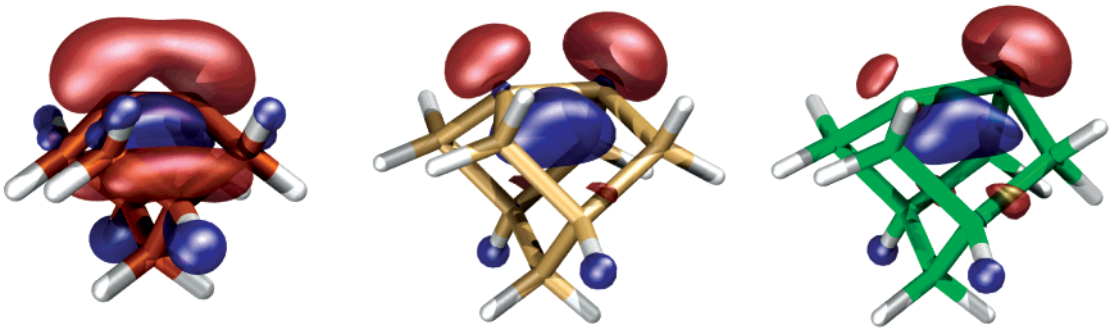

Figure 2. The one dimer clusters used in this work: (a) C_9H_{12}, (b) Si_9H_{12}, and (c) Ge_9H_{12} clusters. Highest occupied molecular orbitals (HOMOs) calculated by DFT are shown.

detail previously.[27] Briefly, the chamber is equipped with an unshielded quadrupole mass spectrometer and an ion gun for surface sputtering. Single crystalline Ge(100) or Si(100) samples were cut into trapezoidal geometry of dimensions 1 × 20 × 50 mm with 45° beveled edges (Harrick Scientific). The crystal was mounted on a holder that is heated by a resistive tungsten heater and cooled by heat exchange with a liquid nitrogen coldfinger. The Ge(100) surface was cleaned in situ by argon ion sputtering at room temperature (6 μA, 0.5 kV) followed by annealing to 900 K for 5 min. This surface preparation procedure routinely produces a smooth Ge(100)-2 × 1 surface, as verified by the presence of sharp monohydride IR features at 1977 and 1988 cm^{-1} after exposure to atomic hydrogen at room temperature.[28] Preparation of the Si(100)-2 × 1 surface follows a similar procedure, as described in detail previously.[13] The back faces of the Si and Ge crystals, which were not cleaned by sputtering, were covered with a thin molybdenum plate to prevent molecular adsorption and surface reaction at the back face.

Infrared spectra of molecules adsorbed on the Ge(100)-2 × 1 and Si(100)-2 × 1 surfaces were collected using an FTIR spectrometer with a liquid-nitrogen cooled HgCdTe detector. The unpolarized beam from the FTIR spectrometer entered and exited the UHV chamber by means of two KBr windows perpendicular to each other. Infrared light was focused onto the beveled edge of the trapezoidal crystal. The IR light propagated and underwent multiple internal reflections inside the crystal. The light emerging from the other beveled edge of the crystal was collected and focused onto the HgCdTe detector. The frequency range of the infrared data was limited by the phonon absorption of the substrates such that vibrational modes below 750 and 1500 cm^{-1} could not be observed on the Ge(100)-2 × 1 and Si(100)-2 × 1 surfaces, respectively. Polarized IR spectra were obtained by inserting a wire-grid polarizer in the IR path before it enters the detector. Spectra in this work were obtained for *p*-polarized light, which probes modes both parallel and perpendicular to the surface, and were corrected for baseline instabilities. The optical path outside the vacuum chamber was purged by dry, CO_2-free air to prevent the occurrence of impurity bands from H_2O and CO_2. For each spectrum, at least 5000 scans were averaged at 4 cm^{-1} resolution. To obtain an absorption spectrum, a background emissivity spectrum of the clean sample was recorded, and subsequent scans after adsorption or reaction were divided by the background spectrum.

TPD experiments were performed in a second stainless steel UHV chamber equipped with an unshielded mass spectrometer (VG), an ion gun for surface sputtering, reverse-view low-energy electron diffraction optics (LEED, Princeton Research Instruments), and a single-pass-cylindrical-mirror analyzer (CMA, Φ 10−155) for Auger electron spectroscopy (AES). A base pressure of less than 1 × 10^{-10} Torr was achieved by using a 220 L/s ion pump (Perkin-Elmer). The Ge(100) sample, of dimensions approximately 15 × 15 mm^2, was cut from single-crystalline Ge(100) wafers (Eagle-Picher). The sample was heated by a resistive tungsten heater and cooled through a copper braid connected to a liquid nitrogen heat sink. Temperature control was achieved by using a digital controller (Eurotherm) coupled to a dc power supply. Following a Ge(100) surface preparation procedure identical to the one used in the IR chamber, the surface reconstruction was confirmed by the appearance of a sharp (100)-2 × 1 LEED pattern, and the surface cleanliness was verified by AES, which showed negligible amounts of carbon and nitrogen. TPD experiments were conducted with a linear temperature ramp of 1 K/s. The sample was positioned line-of-sight to the ionizer of the mass spectrometer, which was approximately 2 in. away. Up to seven masses were recorded simultaneously during each TPD experiment.

Methylamine [NH_2CH_3] (gas, purity 99.5+ %, Matheson), dimethylamine [$NH(CH_3)_2$] (gas, purity 99+ %, Aldrich), and trimethylamine [$N(CH_3)_3$] (gas, purity 99.5+ %, Matheson) were used without further purification, and their purities were verified with use of in situ mass spectrometry. Exposures are reported in units of Langmuir (L), where 1 L = 10^{-6} Torr·s, and the pressures have not been corrected for ion gauge sensitivities. The gases were introduced into the vacuum chambers through variable leak valves. For infrared spectroscopy, exposures were performed by filling the chamber with the compound of interest for a set pressure and time. For TPD experiments, a directed doser, consisting of a leak valve and a stainless steel tube, was used to expose the gases to the sample. The doser consists of a 0.5 in. o.d. tube to provide a directed and uniform gas flux at a distance within 0.125 in. from the surface. The exposures cannot be directly compared in the IR and TPD vacuum systems, since the local gas pressures in the directed tube doser are much higher.

Theoretical Methods

Our theoretical approach was based on density functional theory (DFT)[29,30] with the electronic structure expanded in atomic Gaussian basis functions. A C_9H_{12} one-dimer cluster was used to model the C(100)-2 × 1 surface, while the Si_9H_{12} and Ge_9H_{12} clusters were used to model the Si(100)-2 × 1 and Ge(100)-2 × 1 surfaces, respectively. The one-dimer cluster consisted of two surface atoms representing the surface dimer and seven atoms representing three layers of subsurface bulk atoms. The dangling bonds of the subsurface atoms are terminated by 12 hydrogen atoms to mimic the sp^3 hybridization of the actual surface. The highest occupied molecular orbitals (HOMOs) of the one-dimer clusters calculated by DFT are shown in Figure 2.

The BLYP/6-31G(d) level of theory[31,32] was used to determine the geometries of the critical points on the potential energy surface. All

(27) Kong, M. J.; Lee, K. S.; Lyubovitsky, J.; Bent, S. F. *Chem. Phys. Lett.* **1996**, *263*, 1−7.
(28) Chabal, Y. J. *Surf. Sci.* **1986**, *168*, 594−608.
(29) Hohenberg, P.; Kohn, W. *Phys. Rev.* **1964**, *136*, B864−B871.
(30) Kohn, W.; Sham, L. J. *Phys. Rev.* **1965**, *140*, A1133-A1138.
(31) Becke, A. D. *Phys. Rev. A* **1988**, *38*, 3098−3100.
(32) Lee, C. T.; Yang, W. T.; Parr, R. G. *Phys. Rev. B* **1988**, *37*, 785−789.

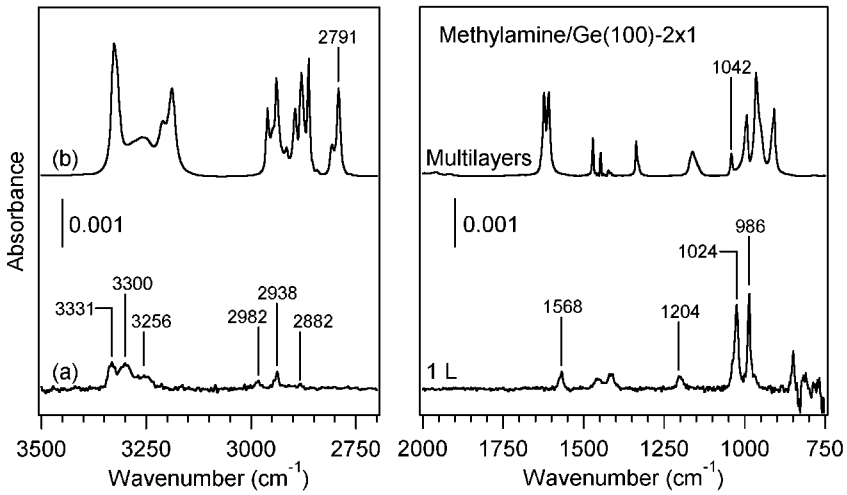

Figure 3. IR spectra of methylamine adsorbed on the Ge(100)-2 × 1 surface: (a) 1 L at 300 K and (b) multilayers condensed at 120 K. The multilayer spectrum is scaled to fit the graph.

structures were fully optimized without geometrical constraints on the clusters, and symmetry restrictions were applied where appropriate. Single-point energy calculations were then performed on the optimized structures at the B3LYP level of theory[32,33] with a mixed basis set scheme. The mixed basis set scheme uses the 6-311++G(d,p) basis set to describe the surface dimer atoms and the amine adsorbate, and the 6-31G(d) basis set to describe the subsurface atoms and the terminating hydrogens. The mixed basis set scheme serves to enhance the accuracy of the electronic structure of the chemically active atoms while minimizing computational costs. The energies reported have been zero-point corrected unless otherwise stated. All electronic structure calculations in this work were performed with the Gaussian 98 suite of programs.[34]

We have shown that our theoretical methods and models are reliable and accurate in predicting semiconductor surface reactions. In particular, we have calculated the reaction of ammonia on the Si(100)-2 × 1 surface using the theoretical methods described above with a Si_9H_{12} cluster[13] and found that our calculated values are consistent with both experimental measurements[35,36] and the detailed theoretical studies by Widjaja and Musgrave.[37,38] In addition, using a Ge_9H_{12} one-dimer cluster, the energy of 1,3-butadiene desorption from the Ge(100)-2 × 1 surface was calculated to be 44.6 kcal/mol at the B3LYP level of theory and a mixed basis scheme[39] very similar to the one used in this work, which compares favorably with TPD measurements.[25] We have also calculated the bond dissociation energies of some Si- and Ge-containing gas-phase species using the highly accurate QCISD(T) method[40] and found good agreement with B3LYP energetics (see Supporting Information).

Results and Interpretation

Identification of Surface Reaction Products. (a) Methylamines on the Ge(100)-2 × 1 Surface. The IR spectrum obtained after exposing a clean Ge(100)-2 × 1 surface to 1 L of methylamine at 300 K is shown in Figure 3a. Similarly, Figures 4a−e and 5a−e show the IR spectra collected after increasing exposures of dimethylamine and trimethylamine on the Ge(100)-2 × 1 surface, respectively. Figures 3b, 4f, and 5f show the IR spectra of the multilayers of methylamine, dimethylamine, and trimethylamine, respectively. Multilayers of unreacted reagents were obtained by condensing the amines onto a cold surface below 120 K in UHV. The spectral assignment of the three compounds is summarized in Table 1. Assignment of the surface infrared spectra was made by comparison to the gas-phase and solid-phase spectra in the literature,[41−44] as well as to vibrational frequencies calculated by DFT. IR peak positions in the chemisorbed spectra of dimethylamine and trimethylamine exhibit little or no dependence on coverage, which suggests that the same primary product is formed as the coverage of the two amines increases. Also, no absorption in the Ge−H stretching vibration region of 1900−2000 cm^{-1} is observed in spectra of chemisorbed methylamine, dimethylamine, or trimethylamine, which shows that neither N−H nor C−H dissociation of amines occurs on the Ge(100)-2 × 1 surface.

Clear evidence is provided in the IR spectra for the retention of the NH_2 group and the N−H bond in chemisorbed methylamine and dimethylamine, respectively. In the spectrum of chemisorbed methylamine (Figure 3a), the vibrational modes at 3331, 3300, 1568, and 1204 cm^{-1} are assigned to NH_2 asymmetric stretch, NH_2 symmetric stretch, NH_2 scissors, and NH_2 bend, respectively. If N−H dissociation of methylamine were the major reaction pathway on the Ge(100)-2 × 1 surface, there would be only one N−H bond in the reaction product. Although N−H stretching and N−H bending vibrations would

(33) Becke, A. D. *J. Chem. Phys.* **1993**, *98*, 5648−5652.
(34) Frisch, M. J.; Trucks, G. W.; Schlegel, H. B.; Scuseria, G. E.; Robb, M. A.; Cheeseman, J. R.; Zakrzewski, V. G.; Montgomery, J. A. J.; Stratmann, R. E.; Burant, J. C.; Dapprich, S.; Millam, J. M.; Daniels, A. D.; Kudin, K. N.; Strain, M. C.; Farkas, O.; Tomasi, J.; Barone, V.; Cossi, M.; Cammi, R.; Mennucci, B.; Pomelli, C.; Adamo, C.; Clifford, S.; Ochterski, J.; Petersson, G. A.; Ayala, P. Y.; Cui, Q.; Morokuma, K.; Malick, D. K.; Rabuck, A. D.; Raghavachari, K.; Foresman, J. B.; Cioslowski, J.; Ortiz, J. V.; Stefanov, B. B.; Liu, G.; Liashenko, A.; Piskorz, P.; Komaromi, I.; Gomperts, R.; Martin, R. L.; Fox, D. J.; Keith, T.; Al-Laham, M. A.; Peng, C. Y.; Nanayakkara, A.; Gonzalez, C.; Challacombe, M.; Gill, P. M. W.; Johnson, B.; Chen, W.; Wong, M. W.; Andres, J. L.; Gonzalez, C.; Head-Gordon, M.; Replogle, E. S.; Pople, J. A. *Gaussian 98*, Revision A.5; Gaussian, Inc.: Pittsburgh, PA, 1998.
(35) Dresser, M. J.; Taylor, P. A.; Wallace, R. M.; Choyke, W. J.; Yates, J. T. *Surf. Sci.* **1989**, *218*, 75−107.
(36) Takaoka, T.; Kusunoki, I. *Surf. Sci.* **1998**, *413*, 30−41.
(37) Widjaja, Y.; Mysinger, M. M.; Musgrave, C. B. *J. Phys. Chem. B* **2000**, *104*, 2527−2533.
(38) Widjaja, Y.; Musgrave, C. B. *Surf. Sci.* **2000**, *469*, 9−20.
(39) Mui, C.; Bent, S. F.; Musgrave, C. B. *J. Phys. Chem. A* **2000**, *104*, 2457−2462.
(40) Pople, J. A.; Head-Gordon, M.; Raghavachari, K. *J. Chem. Phys.* **1987**, *87*, 5968−5975.
(41) Durig, J. R.; Bush, S. F.; Baglin, F. G. *J. Chem. Phys.* **1968**, *49*, 2106−2117.
(42) Buttler, M. J.; McKean, D. C. *Spectrochim. Acta* **1965**, *21*, 465−483.
(43) Goldfarb, T. D.; Khare, B. N. *J. Chem. Phys.* **1967**, *46*, 3379−3384.
(44) Gayles, J. N., Jr. *Spectrochim. Acta, Part A* **1967**, *23*, 1521−1531.

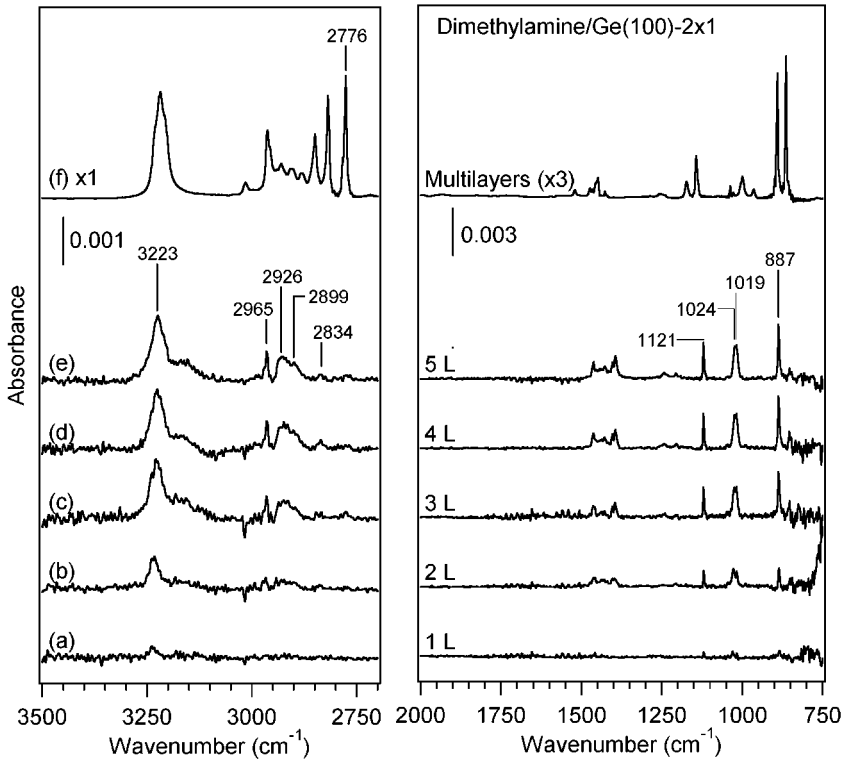

Figure 4. IR spectra of dimethylamine adsorbed on the Ge(100)-2 × 1 surface as a function of exposure: (a) 1, (b) 2, (c) 3, (d) 4, and (e) 5 L at 300 K and (f) multilayers at 120 K.

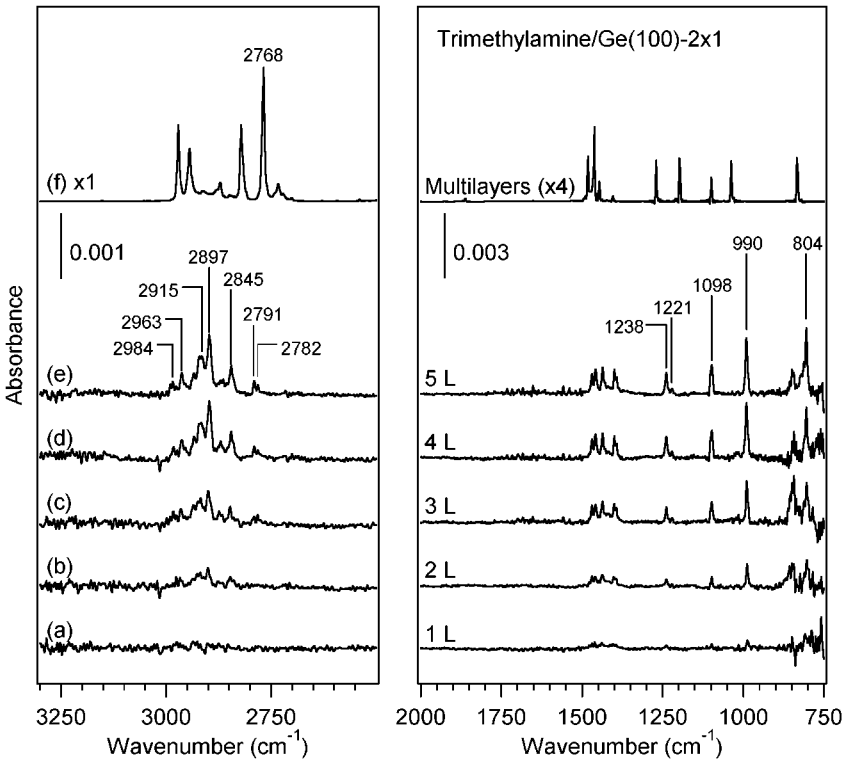

Figure 5. IR spectra of trimethylamine adsorbed on the Ge(100)-2 × 1 surface as a function of exposure: (a) 1, (b) 2, (c) 3, (d) 4, and (e) 5 L at 300 K and (f) multilayers at 120 K.

be observed, the NH_2 scissoring vibration at 1568 cm^{-1} would be completely absent. Similarly, a distinct absorption peak in the N−H stretching region is observed at 3223 cm^{-1} in the spectra of chemisorbed dimethylamine (Figure 4−e), which provides direct evidence for the retention of the N−H bond upon chemisorption.

The IR data also show that the surface reaction of methylamine on the Ge(100)-2 × 1 surface does not involve N−CH_3

Table 1. Infrared Spectral Assignment of Methylamine, Dimethylamine, and Trimethylamine on the Ge(100)-2 × 1 Surface[a]

methylamine	gas phase[41]	multilayers	chemisorption
NH_2 bend	780, 1419	909, 964, 993, 1337	1204
C−N stretch	1044	1042	986
NH_2 scissors	1623	1609, 1622	1568
CH_3 stretch	2820, 2961, 2985	2791, 2807, 2863, 2880, 2895, 2915, 2940, 2961	2882, 2938, 2982
NH_2 stretch	3361, 3427	3189, 3210, 3260, 3327	3300, 3331

dimethylamine	gas phase[42]	multilayers	chemisorption
N−H bend	735, 1455	864, 891, 1522	1019, 1395
C−N stretch	928, 1022	964, 999, 1028, 1038	887
CH_3 stretch	2791, 2806, 2835, 2838, 2852, 2876, 2890, 2914, 2930, 2952, 2959, 2969, 2982	2776, 2784, 2818, 2849, 2882, 2907, 2930, 2942, 2959, 2963	2899, 2926, 2834, 2965
N−H stretch	3355	3015, 3218	3223

trimethylamine	gas phase[43,44]	multilayers	chemisorption
C−N stretch	828, 1275	833, 1269	804, 990
CH_3 stretch	2776, 2953, 2977, 2981	2768, 2822, 2870, 2913, 2944, 2971	2782, 2791, 2845, 2865, 2897, 2915, 2934, 2963, 2984

[a] The frequencies are in units of cm^{-1}. The IR spectra of the multilayers obtained in this work are consistent with the literature.[41−44]

dissociation. In the spectrum of chemisorbed methylamine (Figure 3a), the vibrational mode at 986 cm^{-1} is assigned to a C−N stretch. Note that the 986 cm^{-1} mode is significantly downshifted compared to the C−N stretch of methylamine multilayers at 1042 cm^{-1}. The peak in Figure 3a at 1024 cm^{-1}, although closer to the C−N stretch in the multilayer spectrum, is assigned to a CH_3 rocking mode based on DFT calculations. The downshift of the C−N stretch is expected based on both experimental and theoretical evidence. First, the downshift is consistent with the solid-phase IR spectrum of a model quaternary ammonium ion−methylammonium chloride[45] ($CH_3NH_3^+$ Cl^-), which exhibits a C−N stretch at 1000 cm^{-1}. In addition, our DFT calculations predict that the C−N stretching frequency of methylamine adsorbed on the Ge_9H_{12} cluster is downshifted from that of gas-phase methylamine by 64 cm^{-1}, consistent with the experimentally observed frequency shift of 56 cm^{-1}. The presence of the C−N stretch in the surface reaction product shows that the methyl group is attached to the methylamine molecule after chemisorption. Furthermore, the significant downshift of the C−N vibration upon methylamine chemisorption indicates that the surface reaction product resembles a quaternary ammonium ion.

C−N stretching vibrational modes are also observed in the IR spectra of dimethylamine (Figure 4a−e) and trimethylamine (Figure 5a−e) on the Ge(100)-2 × 1 surface. In the spectrum of chemisorbed dimethylamine, the IR peak at 887 cm^{-1} is assigned to a C−N stretch (Figure 4e). The presence of the C−N stretch shows that at least one N−CH_3 bond of dimethylamine remains intact on the Ge(100)-2 × 1 surface. Direct spectral evidence for the existence of both N−CH_3 bonds upon dimethylamine chemisorption requires the observation of the CNC bending vibration at about 400 cm^{-1}, which is blocked by the strong absorption of the Ge substrate in the multiple internal reflection geometry. For chemisorbed trimethylamine, the peaks at 804 and 990 cm^{-1} are assigned to C−N stretching vibrations (Figure 5a−e). Our IR spectral assignments for dimethylamine and trimethylamine are consistent with the frequencies predicted by DFT. Also, because the observation of an C−N stretch in the methylamine spectrum (Figure 3a) implies that N−CH_3 cleavage on the Ge(100)-2 × 1 surface does not occur to a significant extent, we can deduce that the surface reactions of dimethylamine and trimethylamine on the Ge(100)-2 × 1 surface do not involve N−CH_3 cleavage either. Similar to the surface reaction of methylamine, molecular chemisorption of dimethylamine and trimethylamine results in the formation of a quaternary ammonium ion on the Ge(100)-2 × 1 surface.

Further insights into the electronic structure and bonding configuration of methylamine on the Ge(100)-2 × 1 surface can be obtained by careful analysis of the C−H stretching vibrational modes. For example, intense IR peaks are observed at 2791, 2776, and 2768 cm^{-1} in the multilayer spectra of methylamine (Figure 3b), dimethylamine (Figure 4f), and trimethylamine (Figure 5f), respectively, and these frequencies are unusually low compared to ordinary C−H stretching vibrations. C−H stretching modes of such low frequency, but high intensity, are known as Bohlmann bands. These vibrational modes are attributed to the stretching of C−H bonds oriented *trans* periplanar to the lone pair of the nitrogen atom in an amine molecule. This effect is known as the *trans*-lone-pair effect, in which the interaction between the nitrogen lone pair orbital and the C−H σ-orbital *trans* periplanar to the lone pair causes an increase of C−H bond lengths, and a corresponding redshift in stretching frequencies.[46]

In the IR spectra of chemisorbed methylamine (Figure 3a), dimethylamine (Figure 4a−e), and trimethylamine (Figure 5a−e), C−H stretching modes are observed between 2800 and 3000 cm^{-1}, and IR absorption is highly attenuated at frequencies below 2800 cm^{-1}. This indicates that the lone pair electrons of the amines are involved in bonding to the surface and that they are no longer able to perturb the *trans* C−H bonds of the amine molecule after reaction with the Ge(100)-2 × 1 surface. This analysis of C−H stretching vibrational modes provides strong support that the surface reactions of methylamine, dimethylamine, and trimethylamine at the Ge(100)-2 × 1 surface involve the formation of Ge−N dative bonds, in which both electrons for bond formation are supplied to the Ge(100)-2 × 1 surface by the nitrogen lone pair of the amine molecule. Similar analysis of C−H stretching vibrations has been successfully applied to

(45) Waldron, R. D. *J. Chem. Phys.* **1953**, *21*, 734−741.

(46) McKean, D. C.; Ellis, I. A. *J. Mol. Struct.* **1975**, *29*, 81−96.

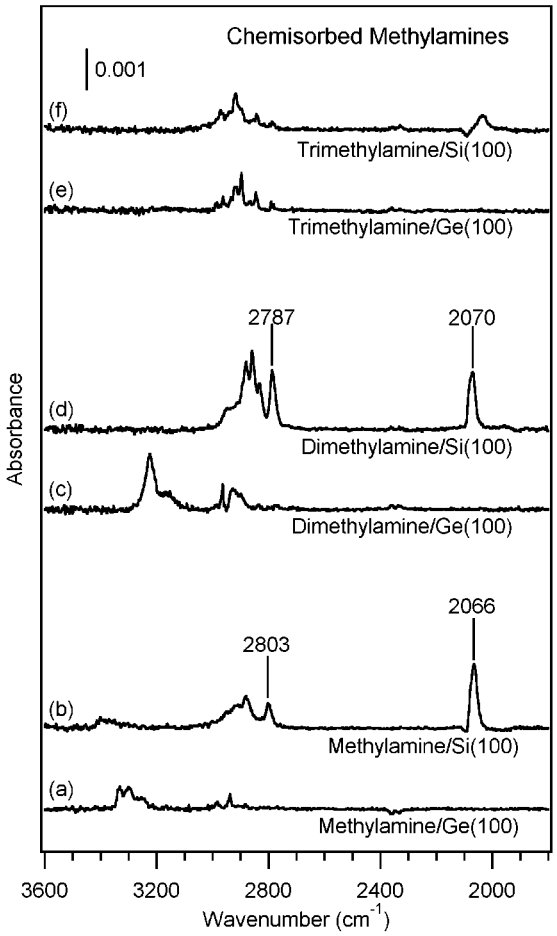

Figure 6. IR spectra of chemisorbed amines on the Si(100)-2 × 1 and Ge(100)-2 × 1 surfaces at saturation coverages: (a) methylamine on Ge(100)-2 × 1, (b) methylamine on Si(100)-2 × 1, (c) dimethylamine on Ge(100)-2 × 1, (d) dimethylamine on Si(100)-2 × 1, (e) trimethylamine on Ge(100)-2 × 1, and (f) trimethylamine on Si(100)-2 × 1.

interpret the surface IR spectra of pyrrolidines[12] and methylamines[13] on the Si(100)-2 × 1 surface.

(b) Methylamines on the Si(100)-2 × 1 Surface. The IR spectra of methylamine, dimethylamine, and trimethylamine at saturation coverages on the Si(100)-2 × 1 surface are shown in Figure 6. Spectra for the Ge(100)-2 × 1 surface are included for comparison. The IR spectra of methylamine and dimethylamine on the Si(100)-2 × 1 surface show Si−H stretching modes at 2066 and 2070 cm^{-1}, respectively (Figure 6b,d). In addition, only a weak N−H stretching mode is observed in the methylamine spectrum at 3043 cm^{-1}, and no N−H stretching vibration is observed in the spectrum of dimethylamine. This indicates that methylamine and dimethylamine undergo N−H dissociation at the Si(100)-2 × 1 surface, resulting in the formation of surface $Si-NHCH_3$(a) and $Si-N(CH_3)_2$(a) species, respectively. In contrast, the spectrum of trimethylamine on the Si(100)-2 × 1 surface (Figure 6f) shows only C−H stretching vibrations, with weak IR absorption in the Si−H stretching region between 2000 and 2100 cm^{-1} most likely due to background contamination.[13] The spectrum of trimethylamine is similar on the Si(100)-2 × 1 and the Ge(100)-2 × 1 surfaces (Figure 6e, f). This indicates that trimethylamine undergoes molecular chemisorption via dative bond formation on both surfaces.

Analysis of the C−H stretching vibrational modes provides further support to the bonding configuration of methylamines on the Si(100)-2 × 1 surface. In the spectra of chemisorbed methylamine and dimethylamine, relatively sharp and intense C−H stretching vibrations are observed at 2803 and 2787 cm^{-1}, respectively. The reappearance of Bohlmann bands upon chemisorption shows that the N lone pair is retained in the reaction product and thus N−H dissociation occurs on the surface. On the other hand, the spectrum of chemisorbed trimethylamine on the Si(100)-2 × 1 surface shows only weak IR absorption in the Bohlmann band region below 2800 cm^{-1}, providing further support for a dative bonded reaction product, in which the lone pair is lost upon chemisorption.

Thermal Desorption of the Chemisorbed Products. Since the adsorption of methylamines on the Ge(100)-2 × 1 surface is molecular and the surface reaction involves the formation of a Ge−N dative bond, TPD can be used to measure the strength of the surface Ge−N bond directly, if reversible desorption of methylamines occurs on the surface. On the Si(100)-2 × 1 surface, detailed thermal studies by Mulcahy et al. showed that dissociation of dimethylamine is the major reaction pathway upon heating.[10] In the present TPD experiments, the Ge(100)-2 × 1 surface was exposed to the amines at 300 K, then the sample was cooled to 180 K before ramping up the temperature. All exposures were chosen to ensure a saturated surface. The desorption products from the Ge(100)-2 × 1 surface were identified by comparing the mass fragmentation patterns of the desorption products to the mass spectra of the gas-phase amines. For example, the TPD spectrum obtained after dosing methylamine onto the Ge(100)-2 × 1 surface showed a mass fragmentation pattern consistent with that of gas-phase methylamine; hence, the desorption product was assigned to molecular methylamine. The TPD spectra of dimethylamine and trimethylamine were assigned in a similar fashion.

TPD spectra of the parent masses of methylamine (*m*/*e* 31), dimethylamine (*m*/*e* 45), and trimethylamine (*m*/*e* 59) are shown in Figure 7. The results indicate that the majority of methylamine, dimethylamine, and trimethylamine desorbs molecularly from the Ge(100)-2 × 1 surface upon heating, resulting in desorption peak temperatures of 345, 360, and 360 K, respectively. However, desorption of trace hydrogen was observed in the TPD spectra of all three methylamines, indicating that dissociation to form surface hydrogen is a minor reaction pathway.

The relative saturation coverages of the adsorbed amines on the Ge(100)-2 × 1 surface can be deduced from the TPD spectra. Straightforward integration of the TPD peak intensities shows that the integrated peak areas follow the order: methylamine > dimethylamine > trimethylamine. However, after correcting for the sensitivity and the fragmentation pattern of the amines as determined in the UHV system used for TPD in this work, we find the saturation coverages of methylamine and dimethylamine to be similar, whereas the saturation coverage of trimethylamine on the Ge(100)-2 × 1 surface is only about 20% of the saturation coverage of methylamine.

Using a simple Redhead analysis[47] with a typical preexponential factor of 10^{13}, the desorption energies of methylamine, dimethylamine, and trimethylamine were all found to be 23 ± 1 kcal/mol. This result suggests that the adsorption states of

(47) Redhead, P. A. *Vacuum* **1962**, *12*, 203-211.

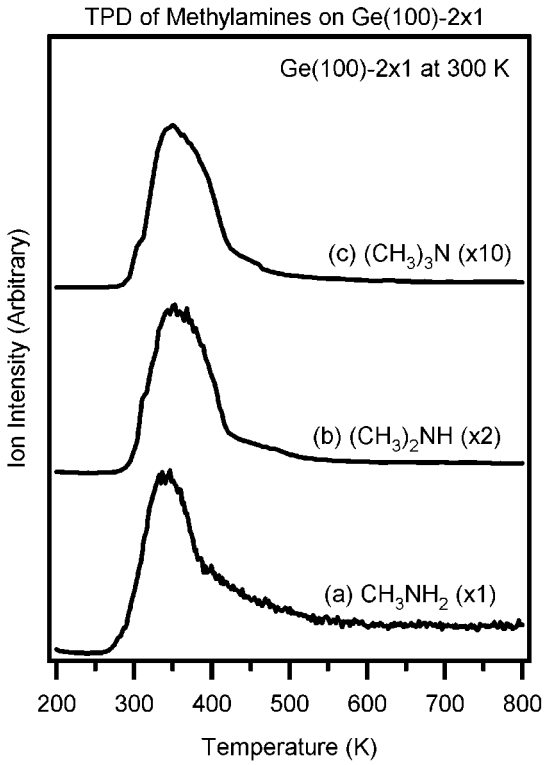

Figure 7. Temperature-programmed desorption spectra of the parent fragment of (a) 0.14 L of methylamine (*m*/*e* =31), (b) 0.05 L of dimethylamine (*m*/*e* 45), and (c) 0.05 L of trimethylamine (*m*/*e* 59) chemisorbed on the Ge(100)-2 × 1 surface. The Ge(100)-2 × 1 surface is exposed to the amines at 300 K.

the three amines at the Ge(100)-2 × 1 surface are similar, and that desorption of each amine occurs by cleavage of the same type of chemical bond. This further supports the conclusion based on the IR spectra that the chemisorptions of methylamine, dimethylamine, and trimethylamine on the Ge(100)-2 × 1 surface all involve the formation of Ge−N dative bonds with the surface. Furthermore, the TPD results quantify the strength of the surface Ge−N dative bond to be about 23 kcal/mol.

Density Functional Theory Calculations. (a) Adsorption Geometries and Energies. DFT calculations can predict the geometries and energies, as well as the vibrational spectra, of the surface reaction products. We have calculated the adsorption energies of methylamine, dimethylamine, and trimethylamine chemisorbed molecularly on the Ge(100)-2 × 1 surface. The highest occupied molecular orbitals (HOMO) of the optimized structures, along with the relative energies of different chemisorption configurations, are shown in Figure 8. We find that all three amines adsorb on the down atom of the Ge−Ge dimer. Two energy minima were identified for the adsorption of methylamine and dimethylamine.

The calculations provide strong evidence for dative bond formation at the Ge(100)-2 × 1 surface upon chemisorption of the methylamines. First, the calculated surface Ge−N bond lengths are significantly longer than Ge−N covalent bonds. For example, the calculated Ge−N bond lengths of the adsorbed methylamines range from 2.13 to 2.18 Å, whereas the experimentally measured[48] Ge−N covalent bond length is 1.70 Å. In addition, the calculated Ge−N covalent bond length for the

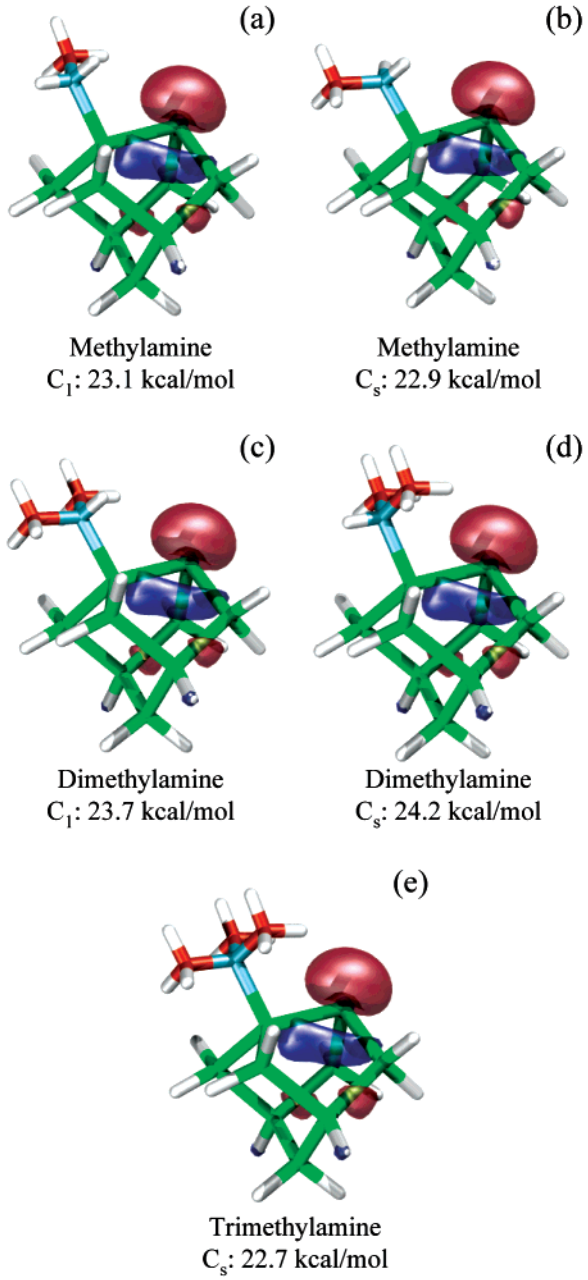

Figure 8. Optimized structures and highest occupied molecular orbital diagrams of dative-bonded amines on the Ge_9H_{12} one dimer cluster: (a) C_1 conformation of adsorbed methylamine, (b) C_s conformation of adsorbed methylamine, (c) dimethylamine C_1 conformation, (d) dimethylamine C_s conformation, and (e) chemisorbed trimethylamine. The numbers are the adsorption energies in kcal/mol.

GeH_3NH_2 molecule is 1.86 Å at the B3LYP/6-311+G(d,p) level. The longer bonds are more consistent with Ge−N dative bonds. Second, the calculations show that the molecular chemisorption of methylamine, dimethylamine, and trimethylamine involves the interaction between the nitrogen lone pair of the amine molecule and the *down* Ge atom of the Ge−Ge dimer. Since the down Ge atom of the Ge−Ge dimer is electron deficient, it readily accepts the electrons of the nitrogen lone pair to form a Ge−N dative bond, in which both electrons of the Ge−N bond are supplied by the nitrogen lone pair.

The calculated adsorption energies show good agreement to the binding energy determined in TPD experiments (Table 2), providing further support that the adsorptions of methylamine,

(48) Riviere-Baudet, M.; Morere, A.; Britten, J. F.; Onyszchuk, M. *J. Organomet. Chem.* **1992**, *423*, C5−C8.

Table 2. Adsorption Energies and Desorption Temperatures of Methylamines on the Ge(100)-2 × 1 Surface Obtained from DFT Calculations and TPD Measurements[a]

adsorption energy	methylamine	dimethylamine	trimethylamine
DFT (C_1 conf.)	−23.1	−23.7	N/A
DFT (C_s conf.)	−22.9	−24.2	−22.7
TPD ($\nu = 10^{13}$)	−23 ± 1	−23 ± 1	−23 ± 1
desorption temp.	345 K	360 K	360 K

[a] All energies are in kcal/mol.

dimethylamine, and trimethylamine at the Ge(100)-2 × 1 surface are all molecular in nature. However, the level of agreement between the calculations and the TPD measurements may be fortuitous because of possible charge-transfer effects. The formation of a dative bond between an amine molecule and the surface dimer involves charge donation from the lone pair of the amine molecule to the surface. Studies by Widjaja and Musgrave on ammonia adsorption at the Si(100)-2 × 1 surface showed that formation of a dative bond involves charge transfer from the ammonia lone pair to the neighboring dimers on the surface, resulting in a stabilization of the dative-bonded state by ∼6 kcal/mol on a three-dimer cluster.[38] Recent X-ray photoelectron spectroscopy (XPS) and natural population analysis (NPA) studies by Cao and Hamers provided quantitative estimates on the atomic charges of the surface Si dimer atoms before and after trimethylamine adsorption, and showed that charge redistribution does occur on the Si−Si dimer upon dative bond formation.[15] If similar nonlocal charge-transfer effects are important for the adsorption of amines on the Ge(100)-2 × 1 surface as for the Si(100)-2 × 1 surface, then the calculated energy may need to be corrected by ∼6 kcal/mol for charge-transfer effects. Further studies will be necessary to probe this issue.

It is interesting to note that the calculated surface Ge−N dative bond strength (23−24 kcal/mol) is very similar to the calculated energy of a Si−N dative bond on the Si(100)-2 × 1 surface (24−25 kcal/mol).[13] In addition, our recent calculations show that the strengths of surface Si−O and Ge−O dative bonds formed by acetone adsorption on the Si(100)-2 × 1 and Ge(100)-2 × 1 surfaces are both 12−14 kcal/mol.[49] These combined results suggest that the nature of the lone pair appears to have a larger influence on the energy of a dative bond than does the identity of the electrophilic atom on the surface.

(b) N−H Dissociation of Dimethylamine. To explore quantitatively the reactivities of group IV semiconductor surfaces toward N−H dissociative adsorption of amines, we have calculated the reaction paths for N−H dissociation of dimethylamine on the Ge(100)-2 × 1, Si(100)-2 × 1, and C(100)-2 × 1 surfaces. The calculated reaction path of dimethylamine adsorption via N−H dissociation on the Ge(100)-2 × 1 surface is shown in Figure 9. Because we have previously shown for the Si(100)-2 × 1 surface that the reaction paths for N−H dissociation are similar for methylamine, dimethylamine, and trimethylamine,[13] here we focus only on dimethylamine on the Ge(100)-2 × 1 surface to illustrate the energetics. Our calculations show that N−H dissociation of dimethylamine occurs via the molecularly chemisorbed state, which has an adsorption energy of 24.2 kcal/mol. The energy of the N−H dissociation transition state is only 0.1 kcal/mol above the vacuum level,

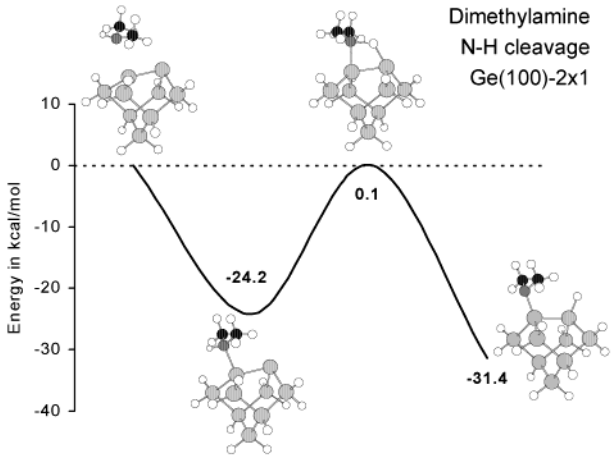

Figure 9. Calculated reaction pathway for N−H dissociation of dimethylamine at the Ge(100)-2 × 1 surface. All energies are with respect to the vacuum level in kcal/mol. The large light gray atoms are Ge, the small black atoms are C, the small white atoms are H and the small dark gray atom is N.

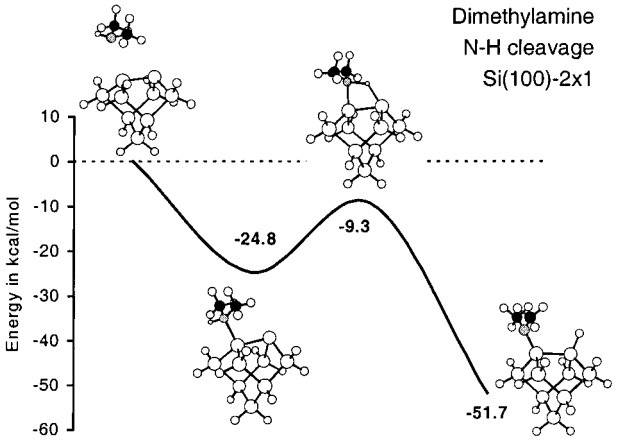

Figure 10. Calculated reaction pathway for N−H dissociation of dimethylamine at the Si(100)-2 × 1 surface. All energies are with respect to the vacuum level in kcal/mol. The large white atoms are Si, the small black atoms are C, the small white atoms are H, and the gray atom is N.

and the overall H-loss process is found to be 31.4 kcal/mol exothermic. N−H cleavage of dimethylamine results in the formation of a surface Ge−N$(CH_3)_2$ species and a Ge−H bond on the surface.

The reaction paths for N−H dissociation of dimethylamine on the Si(100)-2 × 1[13] and C(100)-2 × 1 surfaces are also shown to compare the reaction energetics at group IV semiconductor surfaces. On the Si(100)-2 × 1 surface, dimethylamine first adsorbs onto the down atom of a Si−Si dimer with an adsorption energy of 24.8 kcal/mol (Figure 10). N−H dissociation then proceeds through a transition state, located 9.3 kcal/mol below the vacuum level, to form a surface Si−N$(CH_3)_2$ species and an Si−H bond.[13] The overall exothermicity for N−H dissociation on the Si(100)-2 × 1 surface is 51.7 kcal/mol. We find that the N−H cleavage reaction paths of dimethylamine at the Si(100)-2 × 1 and Ge(100)-2 × 1 surfaces both involve a dative-bonded precursor state. However, the transition state and the reaction products at the Si(100)-2 × 1 surface have lower energies relative to the vacuum level than those at the Ge(100)-2 × 1 surface.

On the C(100)-2 × 1 surface, the C−C dimers are symmetric (Figure 2a) and we find that the formation of a molecularly

(49) Wang, G. T.; Mui, C.; Musgrave, C. B.; Bent, S. F. *J. Phys. Chem. B* **2001**, *105*, 12559−12565.

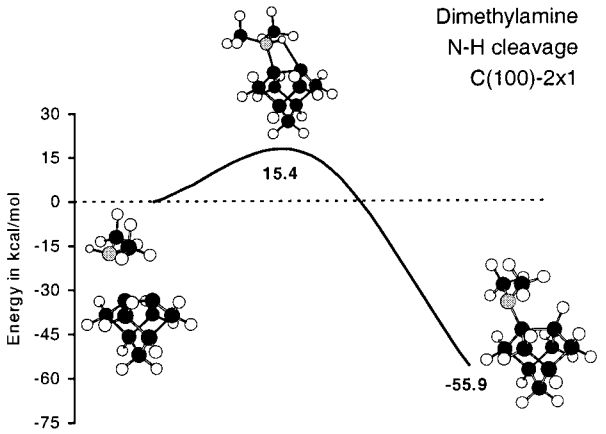

Figure 11. Calculated reaction pathway for N−H dissociation of dimethylamine at the C(100)-2 × 1 surface. All energies are with respect to the vacuum level in kcal/mol. The black atoms are C, the white atoms are H, and the gray atom is N.

adsorbed state between dimethylamine and the C(100)-2 × 1 surface is unfavorable. The calculations show that dimethylamine undergoes direct dissociative chemisorption on the C(100)-2 × 1 surface to form a surface C−N$(CH_3)_2$ species and an C−H bond (Figure 11). The transition state is located 15.4 kcal/mol above the vacuum level, while the overall N−H dissociation is 55.9 kcal/mol exothermic. Since molecular chemisorption of dimethylamine is unfavorable on the C(100)-2 × 1 surface and the energy of the N−H cleavage transition state is significantly above the vacuum level, we predict that dimethylamine will not react on the C(100)-2 × 1 surface.

Discussion

IR spectroscopy on the Si(100)-2 × 1 and Ge(100)-2 × 1 surfaces shows that whereas N−H dissociation is the major reaction pathway for primary and secondary amines on the Si(100)-2 × 1 surface, N−H dissociation is precluded on the Ge(100)-2 × 1 surface. Instead, molecular chemisorption of amines occurs on the Ge(100)-2 × 1 surface through Ge−N dative bond formation. The difference in reactivities between the two group IV semiconductor surfaces can be interpreted as a measure of the proton affinities of the two solid surfaces, since N−H dissociative adsorption of amines on group IV semiconductor surfaces resembles an intradimer proton-transfer process at the surface. According to this description, the proton affinity of the Si(100)-2 × 1 surface is stronger than that on the Ge(100)-2 × 1 surface.

The DFT calculations provide quantitative evidence for the stronger proton affinity observed on the Si(100)-2 × 1 surface. On the Ge(100)-2 × 1 surface, proton transfer from the surface dimethylammonium ion has an activation energy of 24.3 kcal/mol and the overall energy of reaction is only 7.2 kcal/mol exothermic relative to the chemisorbed dimethylammonium state (Figure 9). On the Si(100)-2 × 1 surface, however, the activation energy for proton transfer is only 15.5 kcal/mol and the reaction energy is 27.0 kcal/mol exothermic (Figure 10). Since the up atom of a surface dimer is nucleophilic, the calculations show that the up atom of a Si−Si dimer has a higher proton affinity than the up atom of a Ge−Ge dimer, both energetically and kinetically. This interpretation is consistent with a decrease in the nucleophilicity of group IV surface lone pairs down the periodic table, and agrees with the expected trend for molecular systems, in which lone pair base strength decreases down a group in the periodic table.

Similar to molecular systems, the proton affinity of the Si(100)-2 × 1 and Ge(100)-2 × 1 surfaces is related to the electronic structure of the surface atoms. The nucleophilic up atom of a tilted dimer on the two surfaces resembles a lone pair and consists primarily of s character from the element.[50] Because the radial distribution function of the 4s orbital in Ge has one more spherical node than the 3s orbital in Si, the 4s electrons tend to penetrate further into the Ge core, and spend more time in the inner lobes of the orbital. Furthermore, the atomic radii of Ge and Si are very similar due to the first insertion of the d-block electrons, which have poor shielding ability. This effect is sometimes known as the scandide contraction.[1] Due to the combined effects of penetration and shielding, the electron density near the core region of a 4s orbital in Ge is higher than that of a 3s orbital in Si, whereas the electron density at bonding distances of the Ge 4s orbital is lower compared to that of the Si 3s orbital. This is also consistent with the fact that each 4s electron in Ge experiences an effective nuclear charge of 6.35, whereas each 3s electron in Si only encounters an effective nuclear charge of 4.85 according to Slater's rule. Since the surface lone pair consists of mainly s-character, the electron density at bonding distances to the Ge nucleophile is lower than that a surface Si nucleophile.

The electronic structure of the Si(100)-2 × 1 and Ge(100)-2 × 1 surfaces affects both the energetics and kinetics of surface proton-transfer reactions. First we shall explain the energetics of proton transfer on the two surfaces. To relate the relative stability of the N−H dissociation products on the two surfaces to the bond strengths of gas-phase analogues, we have calculated the bond dissociation energies of some gas-phase species containing Si or Ge using the highly accurate QCISD(T) theoretical method.[40] The calculated Ge−H and Ge−N bond dissociation energies are 82.0 and 82.5 kcal/mol, respectively, whereas the Si−H and Si−N energies are calculated to be 90.6 and 99.8 kcal/mol, respectively (see Supporting Information). The weaker Ge−H bond observed is a direct consequence of the 4s electron density distribution in Ge, such that less electron density is available to form a covalent bond. Assuming the bond dissociation energies of these gas-phase molecules are similar to the bond strengths on the surface, the difference in N−H dissociation reaction energies at the Si(100)-2 × 1 and Ge(100)-2 × 1 surfaces can be explained in terms of bond strength differences. In the proton-transfer process at the Si(100)-2 × 1 surface, the N−H bond is cleaved, and strong Si−N and Si−H covalent bonds are formed on the surface. Similar bond-breaking and bond-forming processes occur during N−H dissociation at the Ge(100)-2 × 1 surface. The exothermicity of a surface reaction can be estimated as the difference between the bond formation energies of the products and the bond dissociation energies of the reactants. Since stronger bonds are formed on the Si(100)-2 × 1 surface after N−H dissociation, the surface reaction on the Si(100)-2 × 1 surface is more exothermic than that on the Ge(100)-2 × 1 surface.

Next we focus on the activation barrier of proton transfer on the Si(100)-2 × 1 and the Ge(100)-2 × 1 surfaces. Figure 12 shows the HOMOs of the transition states for proton transfer on the two surfaces. It is apparent from the HOMO diagrams

(50) Bent, H. A. *Chem. Rev.* **1961**, *61*, 275−311.

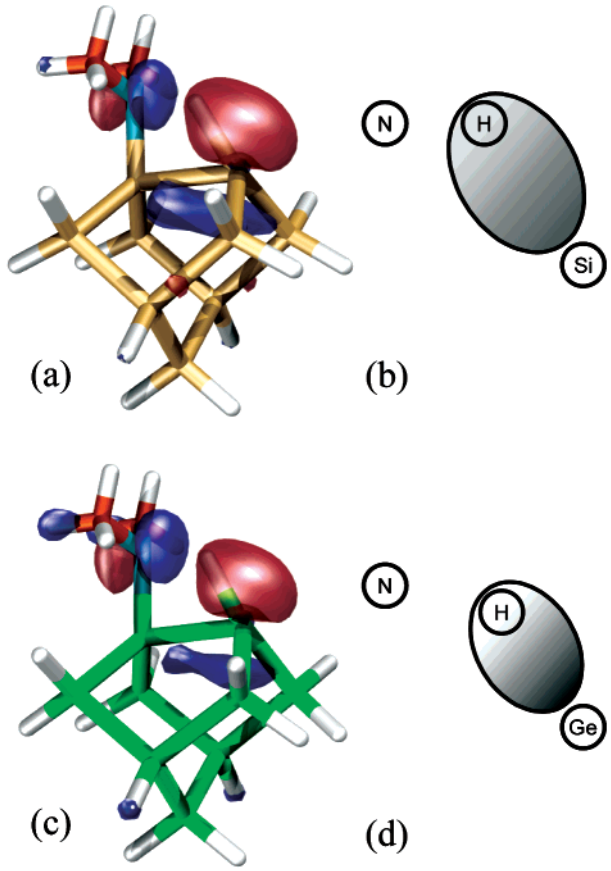

Figure 12. Orbital visualization of the proton-transfer transition states of dimethylamine on the Si(100)-2 × 1 and Ge(100)-2 × 1 surfaces: (a) HOMO diagram of proton transfer on the Si(100)-2 × 1 surface; (b) proton abstraction by nucleophilic Si surface lone pair, which has a higher electron density available for Si−H bond formation; (c) HOMO diagram of proton transfer on the Ge(100)-2 × 1 surface; and (d) proton abstraction by the nucleophilic Ge surface lone pair with a lower electron density for proton abstraction.

that the Lewis-basic up atom of the dimer uses its electron density to interact with the N−H σ-bond from its backside, and abstracts the proton from the adsorbed dimethylammonium ion. The proton abstraction process is facilitated by electron donation from the nucleophilic atom of the dimer to the N−H σ-antibonding orbital, and the interaction is symmetry allowed. Therefore, proton transfer is more favorable if the nucleophilic atom of the dimer has a higher electron density for bond formation.

Since the Ge surface nucleophile has a lower electron density for Ge−H bond formation, abstraction of a proton from the adsorbed amine at the Ge(100)-2 × 1 surface requires that the proton approach closer to the Ge nucleophile such that the proton can acquire enough electron density to form the new Ge−H bond. As a consequence, the N−H bond has to be stretched more at the transition state. The additional stretch of the N−H bond introduces more strain to the transition state for N−H dissociation at the Ge(100)-2 × 1 surface, and raises the activation barrier. This effect can be visualized from the orbital and geometric structures of the transition states shown in Figure 12. The HOMOs of the transition states in Figure 12a, b show that the Ge−H bonding orbital is slightly smaller than the Si−H bonding orbital, which means that the electron density of the Ge nucleophile is lower at the Ge−H bonding distance. This is consistent with the fact that the nucleophilic Ge atom of a Ge−Ge dimer has a lower electron density for proton abstraction compared to the corresponding Si atom of a Si−Si dimer. Also, in the transition state for N−H dissociation of dimethylamine on the Si(100)-2 × 1 surface, the N−H bond is stretched 41% compared to the N−H bond length in the adsorbed state, while the Si−H bond at the transition state is stretched 21% compared to the surface Si−H bond in the dissociated product. On the Ge(100)-2 × 1 surface, the corresponding increases in the N−H and Ge−H bond lengths at the transition state are 53% and 13%, respectively.

The DFT calculations for proton-transfer reactions on the Si(100)-2 × 1 and Ge(100)-2 × 1 surfaces also provide a modern, quantitative view of the Hammond postulate[51] applied to semiconductor surface chemistry. The Hammond postulate states that the activation energy of a reaction increases as the reaction becomes less exothermic. The central idea of the postulate is that the transition state will occur later on the reaction path if the reaction is less energetically favorable, an effect that results in a higher activation energy. Our calculations are consistent with this classic idea of general chemistry. The calculated transition state structures show that the N−H bond is more stretched and the Ge−H bond is less stretched in the proton-transfer transition state on the Ge(100)-2 × 1 surface compared to the corresponding bonds on the Si(100)-2 × 1 surface. This means that the transition state on the Ge(100)-2 × 1 surface is further away from the adsorbed amine reactant and closer to the N−H dissociation product. In other words, the transition state occurs later along the reaction path for proton transfer on the Ge(100)-2 × 1 surface than on the Si(100)-2 × 1 surface. Therefore, the less exothermic proton-transfer reaction at the Ge(100)-2 × 1 surface has a higher activation energy compared to N−H dissociation at the Si(100)-2 × 1 surface

Of course, the different proton-transfer affinities observed on the Si(100)-2 × 1 and Ge(100)-2 × 1 surfaces cannot be generalized to a periodic group trend unless the "surface proton affinity" continues to decrease along group IV elemental surfaces. Our calculations for dimethylamine N−H dissociation on the C(100)-2 × 1 surface show that the applicability of the "surface proton affinity" concept is limited by solid-state effects. In other words, the proton affinity of a group IV elemental surface is related to the geometric and electronic structure of the surface, in addition to the local chemical properties of the surface atoms. The C(100)-2 × 1 surface consists of symmetric dimers (Figure 2a), and the π-bond strength of the surface C−C dimer is estimated to be 12−21 kcal/mol.[52] This bond is much stronger than those for the Si(100)-2 × 1 and the Ge(100)-2 × 1 surfaces, which are estimated to be 2−6 kcal/mol.[53−56] The relatively strong π-bonds of the C−C dimer on the C(100)-2 × 1 surface renders a surface electronic structure such that tilting and charge separation are energetically unfavorable, even with external disturbances such as electron

(51) Lowry, T. H.; Richardson, K. S. *Mechanism and Theory in Organic Chemistry*, 3rd ed.; Harper Collins: New York, 1987.
(52) Hukka, T. I.; Pakkanen, T. A.; D'Evelyn, M. P. *J. Phys. Chem.* **1994**, *98*, 12420−12430.
(53) D'Evelyn, M. P.; Yang, Y. M. L.; Sutcu, L. F. *J. Chem. Phys.* **1992**, *96*, 852−855.
(54) Hofer, U.; Li, L. P.; Heinz, T. F. *Phys. Rev. B* **1992**, *45*, 9485−9488.
(55) Nachtigall, P.; Jordan, K. D.; Sosa, C. *J. Phys. Chem.* **1993**, *97*, 11666−11672.
(56) D'Evelyn, M. P.; Cohen, S. M.; Rouchouze, E.; Yang, Y. L. *J. Chem. Phys.* **1993**, *98*, 3560−3563.

donation from the lone pair of an amine molecule. Therefore, the molecular adsorption of dimethylamine is unfavorable and the dimethylammonium ion does not form on the C(100)-2 × 1 surface. Without the formation of a quaternary ammonium ion on a tilted dimer, the notion of nucleophilicity of the up dimer atom vanishes because the "up atom" does not exist. Hence, direct N−H dissociation of dimethylamine on the C(100)-2 × 1 surface cannot be considered as a surface proton-transfer reaction and the "surface-proton affinity" cannot be probed nor estimated.

Although the direct N−H dissociative adsorption of dimethylamine on the C(100)-2 × 1 surface does not constitute a proton-transfer reaction, the energetics of the overall surface reaction do reflect the local chemical properties of the C atoms on the surface. According to our calculations, the overall energy of direct N−H dissociative adsorption of dimethylamine at the C(100)-2 × 1 surface is 55.9 kcal/mol exothermic. On the other hand, precursor-mediated N−H dissociation of dimethylamine on the Si(100)-2 × 1 surface has an overall energy of reaction of 51.7 kcal/mol with respect to the vacuum level. Even though the C(100)-2 × 1 surface consists of relatively stronger surface π-bonds, N−H dissociation at the C(100)-2 × 1 surface is more exothermic than that at the Si(100)-2 × 1 surface. This is because surface C−H and C−N bonds are stronger than Si−H and Si−N bonds, respectively. Therefore, the local chemical properties of the C atoms are preserved on the C(100)-2 × 1 surface and play a major role in determining the overall exothermicity of the N−H dissociation reaction.

Conclusion

We have studied the surface chemistry of methylamine, dimethylamine, and trimethylamine at the Si(100)-2 × 1 and Ge(100)-2 × 1 surfaces to test the applicability of the "surface proton affinity" concept on group IV semiconductor surfaces. By using MIR-FTIR spectroscopy, we have shown that all three amines undergo molecular chemisorption on the Ge(100)-2 × 1 surface via the formation of surface Ge−N dative bonds, and that cleavage of N−H bonds is suppressed. On the other hand, N−H dissociation of primary and secondary amines is facile on the Si(100)-2 × 1 surface. We have applied the concept of proton affinity to explain the difference in reactivity of methylamines at the Ge(100)-2 × 1 and Si(100)-2 × 1 surfaces. A detailed discussion on the relationship between the proton affinity of the nucleophilic up dimer atom and the overall surface reaction energetics, in terms of exothermicity and activation barrier, was presented. Analogy is drawn between an up atom in a surface dimer and a Lewis basic lone pair on the surface. We conclude that the idea of proton affinity, when applied to group IV semiconductor surfaces, is consistent with the expected trend in lone pair basicity in the periodic table. Finally, our calculations on dimethylamine N−H dissociation at the C(100)-2 × 1 surface show that dative bond formation between dimethylamine and the surface is unfavorable, and dimethylamine can only undergo direct N−H dissociative chemisorption on the C(100)-2 × 1 surface. Although solid-state effects of the C(100)-2 × 1 surface seemed to disrupt the trend in surface proton affinity on group IV elemental surfaces, the local atomic properties of the C atoms on the surface play a large role in determining the reaction energetics of the direct dissociative adsorption process.

Acknowledgment. The authors would like to thank Dr. Henry A. Bent for insightful discussions. S.F.B. acknowledges financial support from the National Science Foundation (Grants DMR 9896333 and CHE 9900041) and from the Beckman Foundations. S.F.B. is a Camille Dreyfus Teacher-Scholar. C.B.M. acknowledges financial support from LSI Logic, IBM, Hewlett-Packard, and the Charles Powell Foundation. This research is also partially supported through computing resources provided by NCSA.

Supporting Information Available: Calculated bond dissociation energies of Si and Ge-containing gas-phase species using B3LYP and QCISD(T) theories (PDF). This material is available free of charge via the Internet at http://pubs.acs.org.

JA0171512